Smart Structures and Systems, Vol. 4, No. 4 (2008) 407-428
DOI: http://dx.doi.org/10.12989/sss.2008.4.4.407

Active feedback control for cable vibrations

Filippo Ubertini*

Department of Structural Mechanics, University of Pavia, Via Ferrata 1, 27100 Pavia, Italy

(Received December 13, 2006, Accepted November 15, 2008)

Abstract. The nonlinear mechanics of cable vibration is caught either by analytical or numerical models. Nevertheless, the choice of the most appropriate method, in consideration of the problem under study, is not straightforward. A feedback control policy might even enhance the complexity of the system. Thus, in order to design a suitable controller, different approaches are here adopted. Devices mounted transversely to the cable in the two directions, close to one of its ends, supply the feedback control action based on the observation of the response in a few points. The low order terms of the control law are, at first, analyzed in the framework of linear models. Explicit analytic solutions are derived for this purpose. The effectiveness of high order terms in the control law is then explored by means of a finite element model(FEM), which accounts for high order harmonics. A suitably dimensional analytical Galerkin model is finally derived, to investigate the effectiveness of the proposed control strategy, when applied to a physical model.

Keywords: shallow cable; feedback control; transfer function; numerical simulations; bifurcations.

1. Introduction

The control of cable vibrations is a timely problem in the structural engineering literature. A very promising active control solution is based on the axial support motion; its effectiveness was analyzed in Susumpow and Fujino (1995), Gattulli, *et al.* (1997), Gattulli and Vestroni (2000) and Pasca, *et al.* (1998). The method is based on the presence of the elongation term in the condensed equation of motion. Adjustments are still in progress for such an approach (Alaggio, *et al*. 2006). Particular attention is devoted to the adequateness of the condensation hypothesis in the controlled case and to the controllability of the anti-symmetric modes. The main challenging aspect of active control, applied to nonlinear cables, is probably represented by the estimation of the cable states, which may require a high number of monitored points or the design of a suitable nonlinear state observer (Faravelli and Ubertini 2007).

The use of passive (Soong and Dargush 1997) and semiactive dampers (Casciati, *et al*. 2006), mounted transversely to the cable, is probably the most applied solution to dampen in-plane vibrations and was investigated in many papers (Pacheko, *et al*. 1990, Li, *et al*. 2004, Wu and Cai 2006, Xu and Yu 1999, Abdel-Rohman and Spencer 2004), among others. Transverse passive viscous dampers were applied to the cables of many cable-stayed bridges, although the damper location is typically restricted in the side of the bridge deck, which actually reduces the damping effect. Active and semiactive dampers were proposed in Johnson, *et al*. (2001) and, more recently, in Zhou, *et al*. (2006). The role of passive and semiactive tuned mass dampers for mitigating the vibration of cables, must also be mentioned. Solutions of this type were investigated in Cai, *et al*. (2006) and Casciati and Ubertini

*E-mail: filippo.ubertini@unipv.it

(2007), among others.

Cables can be modeled as prestressed mono-dimensional elastic continua with no flexural, torsional or shear rigidities (Luongo, *et al*. 1984). A variety of complex phenomena were observed in cable dynamics, as described in the two review articles by Rega (2004) and, more recently, in Srinil and Rega (2007). In particular, the bifurcation of the first in-plane mode into a bi-modal spatial oscillation is worth mentioning (Larsen and Nielsen 2004). Most of the nonlinear instabilities that characterize the cable response are enhanced under internal resonance conditions (Benedettini, *et al*. 1995). As an example, a strong interaction, between the first symmetric and the first anti-symmetric in-plane modes, was observed at the first crossover point (Nayfeh, *et al*. 2002), when the Irvine parameter(Irvine and Caughey 1974) approaches the value $\lambda^2 = 4\pi^2$. Such an interaction was also observed in more common non-resonant cables (Gattulli, *et al*. 1997).

The cable dynamics can be studied through analytical and numerical models, in the framework of small or large displacements. Most of the papers related to this topic use low order analytical models, based on the Galerkin approach (Gattulli, *et al.* 1997). The model is thus described by a system of ordinary differential equations (ODEs), obtained by expanding the displacement functions in the space of the linear cable eigenfunctions and by retaining a certain number of degrees of freedom. The influence of the retained number of modes, on the predicted cable response, was carried out in Arafat and Nayfeh (2003). An alternative approach utilizes numerical simulations based on the finite element method (FEM) and on the direct integration of the equations of motion. A comparison between analytical Galerkin and FEM models, has been pursued in Gattulli, *et al.* (2004). That comparison showed the ability of the FEM procedure to catch most of the coupling and bifurcation phenomena occurring in the cable nonlinear response.

When active or semiactive control is introduced in the system, high order modes may be activated. A multi-step analysis may become necessary in order to analyze the control effectiveness in a simple model, at first, and then to validate it, through numerical simulations, in a large dimensional nonlinear model. In this paper, an active controller for cable vibrations is designed. Two feedback control forces are applied, close to one of the cable anchors. At a first stage of approximation, low order terms of the control law are analyzed in the framework of linear models (Ubertini and Domaneschi 2006). Particularly, analytic solutions are derived based on the transfer function approach (Kolovsky 1996). Afterwards, the control law is enriched by higher order terms and numerical simulations are performed in a suitably dimensional nonlinear FEM model. The control effectiveness is then analyzed under free and forced parametric oscillations, by devoting a special care to the participation of high order modes on the controlled response. With the aim of designing an experimental investigation of the problem, a suspended cable model is arranged and identified. A suitably dimensional Galerkin model of the cable is also derived, since it results particularly suitable for the design of nonlinear state observers to be employed in real time control applications. The effectiveness of the proposed control strategy, applied to the physical model, is finally discussed.

2. Governing relations

2.1. Discrete linear cable model

Let *Oxyz* be a Cartesian references system and $(0, -g, 0)^T$ be the vector of gravity acceleration. The motion of a suspended cable with a sag d and a transverse control action $\mathbf{U}(t)$ can be analyzed through a

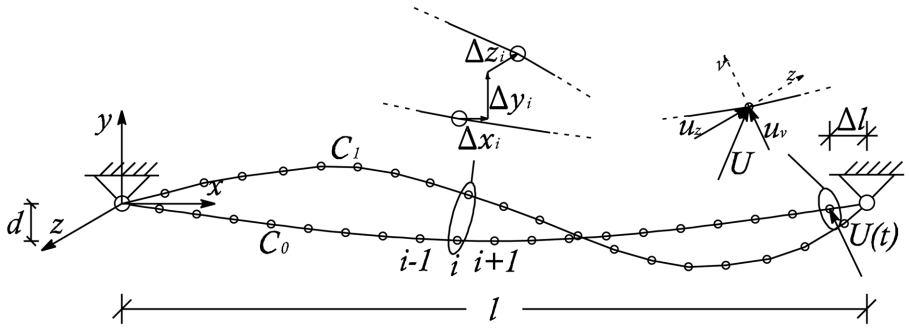

Fig. 1 Discrete cable model with transverse control

discrete approach. The cable is hinged at two supports placed at $(0, 0, 0)^T$, $(l, 0, 0)^T$ respectively. The vibration of the system is then described by the motion of n unconstrained nodes (see Fig. 1), placed at equidistant intervals $\Delta l = \frac{l}{n+1}$ along the x direction. The static configuration C_0 belongs to the Oxy plane and it is assumed as the reference condition. The vector of displacement $Q = (\Delta x_1, \Delta y_1, \Delta z_1, ..., \Delta x_i, \Delta y_i, \Delta z_i, ...\Delta x_n, \Delta y_n, \Delta z_n)^T \in \mathbb{R}^{3n}$ describes the spatial deformed configuration C_1.

The control force $\mathbf{U}(t)$ is applied at the point $(n\Delta l, 0, 0)^T$. It has, in general, an in-plane component $u_v\hat{\mathbf{v}}$ and an out-of plane one $u_z\hat{\mathbf{z}}$, where $\hat{\mathbf{v}}$ and $\hat{\mathbf{z}}$ are the unit-vectors along the v in-plane direction, orthogonal to the cable at $x = n\Delta l$, and along the z direction respectively. This can be achieved by adopting two actuators in the said directions.

Under the hypothesis of small displacements, the motion of the cable can be analyzed in the framework of the linear models. In this case, a convenient representation of the system is sought by expanding the vector of nodal displacements $\mathbf{Q}$ in the space of modal coordinates $\mathbf{q} = \mathbf{\Phi Q}$, where $\mathbf{\Phi} \in \mathbb{R}^{3n\times 3n}$ is the matrix of linear cable eigenvectors, calculated by Irvine's Theory(Irvine and Caughey 1974). The vector of modal displacements is composed as $\mathbf{q} = [q_1^z, q_1^y, q_2^z, q_2^y, ..., q_{3n}^z, q_{3n}^y]$ where q_i^z indicates the i-th out-of-plane coordinate and q_i^y is the i-th in-plane one. By omitting the superscript y, the equation of motion of the i-th in-plane mode can be written as:

$$\ddot{q}_i(t) + 2\xi_i\omega_i\dot{q}_i(t) + \omega_i^2 q_i = f_i(t) + \phi_i^0 u_v(t) \tag{1}$$

where ϕ_i^0 is the component of the i-th in-plane eigenvector at the position of the control force and f_i is the i-th modal-component of the external load. In Eq. (1) ω_i represents the natural circular frequency of the i-th in-plane mode and ξ_i is the modal damping. Similarly, by omitting the superscript z, the equation of motion of the i-th out-of-plane mode reads as Eq. (1), in which u_v is substituted by u_z. Eq. (1) presents all the main features of linear models. In particular the modal coordinated are independent from each other and the cable response can be calculated through the wellknown modes superposition method.

2.2. Cable nonlinear FEM model

The hypothesis of small displacements is usually inadequate to study the dynamics of cables. The equations of motion require therefore to be enriched by geometric nonlinear terms. The easiest way to do so, is to discretize the cable into n+1 tridimensional geometric nonlinear trusses. The equations of motion are then written following the classical *Updated Lagragian* approach:

$$\mathbf{M}\ddot{\mathbf{Q}}(t) + \mathbf{C}\dot{\mathbf{Q}}(t) + (\mathbf{K}_E + \mathbf{K}_T(\mathbf{Q}))\mathbf{Q}(t) = \mathbf{F}(t) + \mathbf{U}(t) \tag{2}$$

where the dots represent the derivatives with respect to time t, $\mathbf{M}$ is mass matrix, $\mathbf{C}$ is the damping matrix and $\mathbf{K}_E$ and $\mathbf{K}_T$ are the elastic and geometric tangent stiffness matrices respectively. The right hand side of Eq. (2) represents the external excitation composed by the vector of nodal forces $\mathbf{F}(t)$ and the vector of control forces $\mathbf{U}(t) = (0, 0, 0,..., U_x, U_y, U_z)^T$, that is a function of the observed variables, as explained in Section 2.1.

Numerical simulations are conducted in Section 4.3. and 4.4. through the nonlinear FEM model described above. The model is coded in the MatLab (The Mathworks Inc 2002) environment. Eq. (2) is integrated in time through the implicit Hilber-Hughes algorithm with the introduction of a scalar parameter for controlling the numerical damping of higher modes without reducing the algorithm accuracy (Hilber, *et al.* 1977). The iterative Newton-Raphson scheme is adopted to calculate the solution at time $t + \Delta t$, once the solution at time t is known. This is achieved by adopting a linear initial estimate of the vector of restoring forces $\mathbf{R}(t + \Delta t, \mathbf{Q}) = (\mathbf{K}_E + \mathbf{K}_T(\mathbf{Q}(t + \Delta t)))\mathbf{Q}(t + \Delta t)$ as a function of the displacement increments $\Delta\mathbf{Q} = \mathbf{Q}(t+\Delta t) - \mathbf{Q}(t)$:

$$\mathbf{R}(t + \Delta t, \mathbf{Q}) = \mathbf{R}(t) + (\mathbf{K}_E + \mathbf{K}_T(\mathbf{Q}(t)))\Delta\mathbf{Q} \tag{3}$$

Eq. (3) is substituted into Eq. (2) and the vector of displacement increments $\Delta\mathbf{Q}$ is calculated iteratively until the error ε^k at the k-th iteration satisfies:

$$\varepsilon_k = \sqrt{\left| \frac{\delta\mathbf{Q}^{k^T}\delta\mathbf{Q}^k}{\mathbf{Q}^{k^T}\mathbf{Q}^k} \right|} < \tilde{\varepsilon} \tag{4}$$

where $\Delta\mathbf{Q} = \sum_{i=1}^{k}\delta\mathbf{Q}^i$. The parameters of the time integration scheme are selected so as to achieve convergence for any time step Δt and to gain a high numerical accuracy(in the following computations one adopts $\Delta t = 0.001s$ and $\tilde{\varepsilon} = 5\cdot10^{-5}$)

A total number of 21 nodes is considered to discretize the cable. The two end nodes are fixed and the 3 degrees of freedom for each the remaining 19 nodes lead to a 57 degrees of freedom system. The large dimension of the model is justified by the need of detecting possible control spillover in high order modes. The initial static configuration C_0 is preliminary calculated and it is achieved by assigning the self-weight to the nodes, in a quasi-static way, starting from a parabolic shape. This basic step is performed in a total time $T > 10T_1$, where T_1 is the period of the first in-plane cable mode. The mid-span vertical increment of sag, with respect to the initial parabolic shape, is corrected by assigning a horizontal small displacement to one of the supports, in a quasi-static way, in a further total time T. The preliminary phase has therefore a total duration $2T$ which corresponds to $2T/\Delta t$ integration steps. A conventional damping matrix $\mathbf{C} = 2\mathbf{M}$ is assumed in such a preliminary phase, in order to reach the static solution with zero nodal velocities and accelerations. A Rayleigh damping matrix $\mathbf{C} = \alpha\mathbf{M}+\beta\mathbf{K}$ is considered after the preliminary phase.

Eq. (2) preserves all the features of nonlinear cable dynamics. In particular, as expected, the independence of the modes is lost due to nonlinear modal coupling terms. As an example, in the nonlinear case, an out-of-plane motion is always coupled with an in-plane one. However, if the control action is effective in reducing the cable displacements, the modal coordinates still give a significant description of the motion and can be employed in a feedback controller.

2.3. Linearized cable FEM model

The linear case described in Section 2.1. can be interpreted as the linearization of the FEM model described in Section 2.2. This is obtained by adopting a constant stiffness matrix $\mathbf{K}=\mathbf{K}_E+\mathbf{K}_T^0$, where $\mathbf{K}_T^0$ is the tangent geometric stiffness matrix calculated at the static configuration C_0. Matrix $\mathbf{\Phi}$ and the natural circular frequencies ω_i can be calculated by eigenvalue analysis. In particular matrix $\mathbf{\Phi}$ is normalized in such a way that $\mathbf{\Phi}^T\mathbf{M}\mathbf{\Phi}=\mathbf{I}$, where $\mathbf{I}$ is the identity matrix. The Rayleigh damping matrix $\mathbf{C}_0=\alpha\mathbf{M}+\beta\mathbf{K}_0$ is adopted and the modal damping terms $2\xi_i\omega_i$ are placed along the main diagonal of matrix $\mathbf{\Phi}^T\mathbf{C}_0\mathbf{\Phi}$.

2.4. Reduced order Galerkin model

The FEM model described in Section 2.2. should be regarded as an accurate numerical tool, in the sense that it consideres high order harmonics in a geometric nonlinear framework and applies to arbitrarily sagged cables. Moreover, the adopted time integration scheme is implicit, which is essential to guarantee numeric stability, and second-order accurate, which means that the integration error grows as the step to the power of 3. An alternative approach is represented by the Galerkin method applied to the equations of motion of the continuous model. Such a method is very wellknown in the literature and the model can be built following standard rules. With such an approach, one expands the cable displacement functions on a suitable base, which usually is composed by the linear cable eigenfunctions. By retaining $\bar{k}$ and $\bar{m}$ in-plane and out-of-plane degrees of freedom, the model of a shallow (parabolic) cable, assumes the following general form (Gattulli, *et al.* 2004):

$$\begin{aligned} \ddot{q}_i^y + \xi_i^y \dot{q}_i^y + \sum_{j=1}^{\bar{k}} a_{0ij} q_j^y + (a_{1i} + \sum_{j=1}^{\bar{k}} a_{2j} q_j^y)\bar{e} &= \theta_{iv}(t), \quad i = 1, ...\bar{k} \\ \ddot{q}_i^z + \xi_i^z \dot{q}_i^z + \omega_{iz}^2 q_i^z + a_{3i} q_i^z \bar{e} &= \theta_{iw}(t), \quad i = 1, ..., \bar{m} \end{aligned} \tag{5}$$

As it is wellknown the hypothesis of parabolic cable requires a small sag to span ratio, which is often the case in structural applications. The control forces have been introduced in Eq. (5) by means of their normalized modal components $\theta_{iv}(t)$ and $\theta_{jw}(t)$. The constant elongation term, in Eq. (5), is denoted by $\bar{e}$ and it is defined as:

$$\bar{e} = \sum_{j=1}^{\bar{k}} b_{1j} q_j^y + \sum_{i=1, j=1}^{\bar{k}} b_{2ij} q_i^y q_j^y + \sum_{s=1}^{\bar{m}} b_{3s} q_s^{z2} \tag{6}$$

where the coefficients a_{0ij}, a_{1j}, a_{2j}, a_{3i}, b_{1j}, b_{2ij}, b_{3s} depend upon the cable mode shapes.

Using small dimensional analytic models allows to gain fast numerical integrations and gives the chance to build nonlinear state observers to be employed in real control applications with minimal number of nodal observations (Faravelli and Ubertini 2007). To this end, the results obtained by means of the larger dimensional FEM model can give indications on the adequateness of the dimension of the Galerkin model (Gattulli, *et al.* 2004). In particular, a Galerkin model with 4 in-plane and 4 out-of-plane degrees of freedom is coded in the MatLab environment, since it gives an accurate description of the multimodal controlled cable dynamics, as discussed in section 5. The model is integrated in time by means of a Runge Kutta method of order 4, with a global error tolerance of 10^{-6}.

3. Control strategy

A control algorithm is proposed to reduce the spatial cable vibrations. The technical relevance of the problem is justified by the need of reducing the risk of fatigue ruptures, which are a likely occurrence in structural cables (Cluni, *et al.* 2007). The effectiveness of derivative terms in the first two modes is analyzed, in the linear case, in Section 4.2. To this end, explicit solutions are derived under free spatial vibrations. The calculations are reported in Appendix. The hypothesis of perfect observability of the two modes is retained in the linear case. The computational FEM approach to the nonlinear case, shows that, as the vibration amplitudes increase, more terms are necessary in the control law in order to get a high control effectiveness. Proportional and derivative terms on the first four in-plane and out-of-plane modes are then introduced in the control law. Numerical simulations are conducted in Section 4.3. and 4.4. to investigate the control effectiveness in the framework of large displacements. Five nodal observations are seen to be necessary to prevent control spillover. On the basis of the presented results, the Galerkin model is validated is Section 5.1. Afterwards, the reduced model is applied to a physical cable arranged in the laboratory environment and preliminary identified in Section 5.2. Numerical simulations are then conducted, in Section 5.3., to investigate the harmonic solutions of the system, under in-plane and out-or-plane loading.

3.1. Linear case

The control devices are placed at a distance $\Delta l = 0.05l$ from one anchor. Such a distance is sufficiently small to attach the control devices to the deck or to the vertical support of the cable, in a typical structural context. In order to introduce an additional damping in q_1^y and q_1^z, a modal derivative(MD) controller is designed as:

$$\begin{aligned} u_v(t) &= -g_{d1}^y \cdot \dot{q}_1^y(t) \\ u_z(t) &= -g_{d1}^z \cdot \dot{q}_1^z(t) \end{aligned} \tag{7}$$

where g_{d1}^y and g_{d1}^z are user-defined control gains. The motion of the first in-plane and out-of-plane modes, with the MD controller, can be obtained by substituting Eq. (7) into Eq. (1):

$$\ddot{q}_1(t) + (2\xi_1\omega_1 + \phi_1^0 g_{d1})\dot{q}_1(t) + \omega_1^2 q_1 = f_1(t) \tag{8}$$

Eq. (8) shows that the control action enters the first in-plane and out-of-plane modes as an additional damping. Nevertheless, in the higher modes, it enters as an external force, which might even increase their response. In particular, u_z enters as the out-of-plane modes and u_v enters the in-plane ones. Therefore, a compromise has to be searched in order to find an optimum set of control parameters. For the higher modes an equation of the following type holds true:

$$\ddot{q}_j(t) + 2\xi_j\omega_j\dot{q}_j(t) + \omega_j^2 q_j = f_j(t) - \phi_j^0 g_{d1}\dot{q}_1(t) \tag{9}$$

where $1 < j \leq 3n$.

Eq. (8) can be written in the frequency domain:

$$\tilde{q}_1(s) = \frac{w_1(s)}{1 + w_1(s)w_{c1}(s)} \tilde{f}_1(s) = W_1^c(s)\,\tilde{f}_1(s) \tag{10}$$

where the tilde indicates the Laplace transform and s is the Laplace variable. The term $w_1(s)$ in Eq. (10), is the uncontrolled transfer function between the first modal amplitude and the correspondent modal load component. It can be expressed by the following equation:

$$w_1(s) = \frac{1}{s^2 + 2\xi_1\omega_1 s + \omega_1^2} \tag{11}$$

The feedback transfer function $w_{c1}(s)$ is also introduced in Eq. (10). It is defined as the ratio between the control action and the modal amplitude, in the frequency domain, and it is given by:

$$w_{c1}(s) = \phi_1^0 g_{d1} s \tag{12}$$

The term $W_1^c(s)$ in Eq. (10) is the closed-loop transfer function of the system composed by the cable mode and the modal control action, as illustrated in Fig. 2. The equations of motion of the higher modes ($1 < j \le 3n$), in the frequency domain, can now be written as:

$$\tilde{q}_j(s) = w_j(s)\tilde{f}_j(s) - w_{cj}(s)\tilde{q}_1(s) \tag{13}$$

where $w_{cj}(s)$ is given by the following equations:

$$w_{cj}(s) = \phi_j^0 g_{d1} s \tag{14}$$

The first mode with MD control is asymptotically stable as long as the poles of the closed loop transfer function $W_1^c(s)$ have strictly negative real parts. By looking at Eq. (8), one can easily observe that $W_1^c(s)$ is simply the transfer function of a second system with circular frequency ω_1 and damping $2\xi_1\omega_1 + \phi_1^0 g_{d1}$. Thus, the stability condition of the system reads as:

$$\phi_1^0 g_{d1} > -2\xi_1\omega_1 \tag{15}$$

3.2. Nonlinear case

A more general modal-proportional-derivative(MPD) control law is adopted, in the nonlinear case. Four in-plane and four out-of-plane modes are considered in the MPD controller, including proportional terms, which enhance the effect of the derivative ones. The control forces are then calculated as:

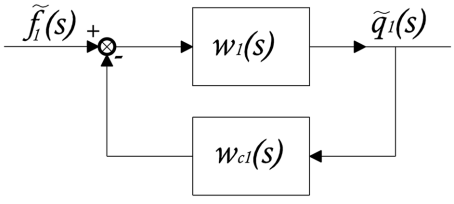

Fig. 2 Closed loop system illustrating Eq. (10)

$$u_v(t) = -\sum_{i=1}^{4}(g_{pi}^{y} \cdot \bar{q}_i^{y}(t) + g_{di}^{y} \cdot \dot{\bar{q}}_i^{y}(t))$$
$$u_z(t) = -\sum_{i=1}^{4}(g_{pi}^{z} \cdot \bar{q}_i^{z}(t) + g_{di}^{z} \cdot \dot{\bar{q}}_i^{z}(t)) \quad (16)$$

where the over-bar indicates an estimate based on the observed variables. Without adopting a nonlinear state observer, a simple estimate $\overline{\mathbf{Q}}$ of the vector of nodal positions is obtained through a "not a knot" cubic spline, that interpolates the nodal observations. The estimate of the vector of nodal velocities $\dot{\overline{\mathbf{Q}}}$, is instead obtained by linear interpolation. With such an approach, five observed points are considered and placed at distance $l/6$, $l/3$,... and $5l/6$ from the anchor at $(0, 0, 0)^T$. The vertical and horizontal displacements of those points are monitored at any time step. The nodal vector $\mathbf{U}(t)$ of control forces, corresponding to Eq. (16), is calculated as:

$$\mathbf{U}(t) = \mathbf{G}_p\overline{\mathbf{Q}} + \mathbf{G}_d\dot{\overline{\mathbf{Q}}} = \begin{bmatrix}\mathbf{G}_p \\ \mathbf{G}_d\end{bmatrix}\begin{bmatrix}\overline{\mathbf{Q}} \\ \dot{\overline{\mathbf{Q}}}\end{bmatrix} = \mathbf{L}\begin{bmatrix}\overline{\mathbf{Q}} \\ \dot{\overline{\mathbf{Q}}}\end{bmatrix} \quad (17)$$

where matrices $\mathbf{G}_p$ and $\mathbf{G}_d$ are defined as:

$$\mathbf{G}_d = \mathbf{\Phi}^{-1}\begin{bmatrix} & 0 & \\ g_{d1}^{z} & g_{d1}^{y} \ldots g_{di}^{z} & g_{di}^{y} \; g_{d4}^{z} \; g_{d4}^{y} \; 0 \ldots 0\end{bmatrix} \quad (18)$$

$$\mathbf{G}_p = \mathbf{\Phi}^{-1}\begin{bmatrix} & 0 & \\ g_{p1}^{z} & g_{p1}^{y} \ldots g_{pi}^{z} & g_{pi}^{y} \; g_{p4}^{z} \; g_{p4}^{y} \; 0 \ldots 0\end{bmatrix} \quad (19)$$

It is worth noting that matrices $\mathbf{G}_d$ and $\mathbf{G}_p$ calculated by Eqs. (18) and (19), have the only non-zero terms along the rows $3n$, $3n-1$, and $3n-2$, that correspond to the degrees of freedom in which the control action is applied.

The optimal gain matrix $\mathbf{L} \in \mathbb{R}^{6n}$, in Eq. (17), is calculated through a linear quadratic regulator (LQR) applied to the linearized system. The gains of the MPD controller are then obtained by retaining the values corresponding to the modes of interest from matrix $\mathbf{L}$. As it is wellknown, from linear control theory, LQR control guarantees asymptotic stability for the linear system, if the controllability condition holds and the weight matrix Q, that appears in the Riccati equation, is properly chosen. Nevertheless, it must be mentioned that, even if designed for linear systems, the LQR regulator is often stabilizing also for nonlinear ones. However, no proof of this result exists, even if the gain matrix is assumed to be state-dependent and it is calculated in real time in the neighborhood of the actual state. Thus, a constant gain matrix is here assumed, in order to minimize the computational expense. The weight matrix $\mathbf{P} = [\mathbf{K}\ 0; 0\ 100\mathbf{M}]$, is considered in the Riccati equation, where $\mathbf{K}$ is the static stiffness matrix, introduced in Section 2.1. As already observed, only the first four in-plane and out-of-plane modes are retained in the control algorithm since observation error increases in higher order modes. The stability of the system must be therefore numerically checked in the large dimensional FEM model, including higher harmonics.

4. Numerical example

4.1. The preliminary case study

The results described in Section 4.2., 4.3. and 4.4. are referred to a sample cable C^1 with the following non-dimensional parameters: $\mu = EA/H = 10970$ and $\nu = d/l = 0.0064$, where E is the Young modulus, A is the cross section and H is the static horizontal reaction at the anchor point. The indicated parameters μ and ν correspond to the stiffness non-dimensional Irvine parameter $\lambda^2 = 2.91\pi^2$. Since $\lambda^2 < 4\pi^2$, cable C^1 is on the left of the first crossover point. This means that the first in-plane symmetric mode has a frequency $f_{1s}{}^y$ that is lower than the frequency of the first anti-symmetric mode $f_{1a}{}^y$ and that the cable remains in tension for any amplitude of vibration.

The first 8 natural frequencies of cable C^1 are obtained numerically, by eigenvalue analysis, at the static configuration C_0. Those values are compared to the analytical ones, calculated by Irvine's Theory (Irvine and Caughey 1974), in Table 1. The frequencies are normalized to the first in-plane eigenfrequency $f_{1s}{}^y = 3.933$Hz. The presented results evidence, as expected, the good accordance between numeric and analytical values. The Rayleigh damping matrix of cable C^1 is calculated with the values $\alpha = 0.027$ and $\beta = 0.0004$, which correspond to the modal damping ratios reassumed in Table 2.

In the following developments, the results will be often reffered to $v_m(t)$ and $w_m(t)$, which are defined as the mid-span vertical and out-of-plane displacements, normalized to the cable span l. The power spectral density function(PSD) of v_q and w_q will also be considered, where v_q and w_q indicate the quarter-span displacements.

4.2. Linear free vibrations

Let us consider, in the linear model, the case of impulsive forces acting simultaneously at each node of the cable in the y and z directions at time $t = 0$. A free motion, mainly composed by the first symmetric in-plane and out-of-plane modes, will then take place for $t > 0$. From a mathematical point of view this corresponds to the application of Dirac-delta nodal forces with the value $A_\Delta \delta(t)$, where A_Δ is the amplitude of the single impulses. The problem is analytically solved in Appendix, where the

Table 1 Natural frequencies of cable C_1 normalized to the first in-plane natural frequency $f_{1s}{}^y = 3.933$Hz

In-plane modes	Analytical	F.E.M.	Out-of-plane modes	Analytical	F.E.M.
$\hat{f}_{1s}^{y}$	1.000	1.002	$\hat{f}_{1s}^{z}$	0.556	0.557
$\hat{f}_{1a}^{y}$	1.113	1.118	$\hat{f}_{1a}^{z}$	1.113	1.118
$\hat{f}_{2s}^{y}$	1.701	1.711	$\hat{f}_{2s}^{z}$	1.669	1.685
$\hat{f}_{2a}^{y}$	2.226	2.264	$\hat{f}_{2a}^{z}$	2.226	2.263

Table 2 Modal damping ratios of cable C_1 corresponding to Rayleigh damping matrix ($\alpha = 0.027$, $\beta = 0.0004$)

1*s*	0.0109	1*s*	0.0073
1*a*	0.0119	1*a*	0.0119
2*s*	0.0175	2*s*	0.0173
2*a*	0.0228	2*a*	0.0228

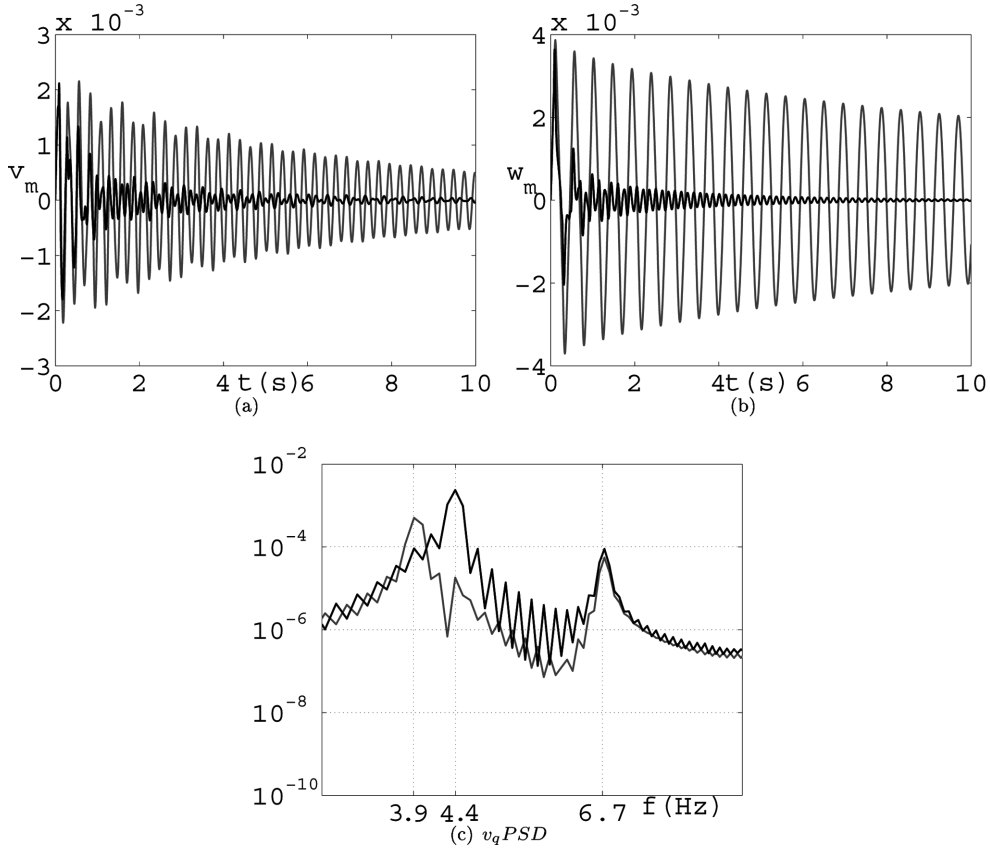

Fig. 3 Analytic solutions for spatial linear free vibrations (uncontrolled in grey, controlled in black)

uncontrolled and controlled solutions are calculated by modes superposition method.

Fig. 3(a) shows the cable normalized in-plane displacement $v_m(t)$, under free vibrations, for a given value A_Δ. Fig. 3(b) shows the normalized out-of-plane displacement $w_m(t)$, under the same conditions. The uncontrolled solution is calculated, as described in Appendix, through Eq. (22), while the controlled one is calculated through Eqs. (23) and (25).

The MD controller introduces, as expected, an additional damping in the first in-plane and in the first out-of-plane cable modes. Such a damping is proportional to the control gains g_{d1}^{y} and g_{d1}^{z}. At the same time, the control action represents a disturbance in the higher modes. This aspect is pointed out in Fig. 3(c), which represents the PSD of v_q. The uncontrolled solution mainly posses the frequencies of the first in plane mode ($f = 3.93Hz$) and of the third one ($f = 6.73Hz$). In the controlled case the first in-plane mode is damped out, but the motion of the second in-plane mode arises ($f = 4.37Hz$). This aspect might even become more relevant when nonlinearities take place, due to coupling phenomena. In order to introduce an additional damping in the first four in-plane and four out-of-plane modes, the control law must be therefore enriched by additional terms. The MPD controller is adopted for this purpose and its effectiveness is analyzed in Section 4.3., 4.4. and 5., through numerical simulations, in the framework of large displacements.

Table 3 Analysis cases for nonlinear free oscillations

Case	*A*	*B*	*C*	*D*
$q_1^{y0}/l \cdot 10^{-3}$	0.7	0.0	0.4	1.6
$q_1^{z0}/l \cdot 10^{-3}$	0.2	1.2	2.3	0.2

4.3. Computational approach to nonlinear free vibrations

The nonlinear FEM model described in Section 2.2. is here adopted and numerical simulations are performed in order to analyze the effectiveness of MPD control algorithm in the case of cable C^1. The free in-plane and out-of-plane vibrations are considered, at first, at different modal amplitudes. Four distinct cases are analyzed, with the in-plane and out-of-plane initial conditions q_1^{y0} and q_1^{z0} assigned to the first two modes, as reassumed in Table 3. Small non-zero initial conditions are also assigned to higher modes which may be involved in the motion due to nonlinear coupling phenomena.

The most significant results of the free vibration analysis are represented in Fig. 4. The main modes that take part to the motion are detected through the PSD of v_q and w_q. At small vibration amplitudes the cable behavior is approximately linear. This means, for instance, that only the modes with non-zero initial conditions are involved in the motion. The considered simulations are performed in such a way that cases *A* and *B* are approximately in the linear field, while cases *C* and *D* involve larger displacements, thus enhancing the nonlinear phenomena. Out of plane bifurcation is not observed in case *A* and out-of-plane displacements in cases *B* and *C* are prevalent with respect to in-plane ones.

Fig. 4 shows that a considerable additional damping is introduced in the system, by MPD control algorithm, in both in-plane and out-of-plane modes. Moreover the control effectiveness seems to be independent from the amplitudes of vibration. Case *D* is of particular interest and the results concerning such a case are analyzed in Fig. 4 with higher detail. Fig. 4(f) shows that the second and the third in-plane modes ($f_2^y = 4.37$ Hz, $f_3^y = 6.68$Hz) also participate to the motion. Moreover, a relevant spatial oscillation occurs in the same case, as observable in Fig. 4(e). Fig. 4(g) shows that such a motion is mainly concerning the first out of plane mode ($f_1^z = 2.18$ Hz). This is probably due to the bifurcation of the first symmetric in-plane mode into a bi-modal spatial oscillation. Finally, Figs. 4(f) and (g) show that the first three peaks of the PSD of v_q and w_q are smoothed in the controlled case. This confirms the ability of the control action to introduce an additional damping in the modes retained in the control law. It must be also mentioned that, in the presented results, five nodal observations and the use of eight modes in the controller prevent control spillover from occurring. Less terms, on the contrary, are seen to determine control spillover at large vibration amplitude.

4.4. Computational approach to nonlinear harmonic vibrations

Three relevant cases of harmonically forced oscillations are considered, as reassumed in Table 4. The external excitation is represented by the horizontal harmonic motion of one support $\Delta_{x0}(t)$ (parametric excitation), having amplitude $\tilde{\Delta}_{x0}l/\mu$ and circular frequency ω. It can be recognized that $\tilde{\Delta}x_0$ represents the ratio between the axial tension induced by a static displacement $\tilde{\Delta}_{x0}l/\mu$ and the static value H_0. The value ω_1^y, in Table 4, indicates the natural circular frequency of the first in-plane symmetric mode ($\omega_1^y = 24.7$ Hz).

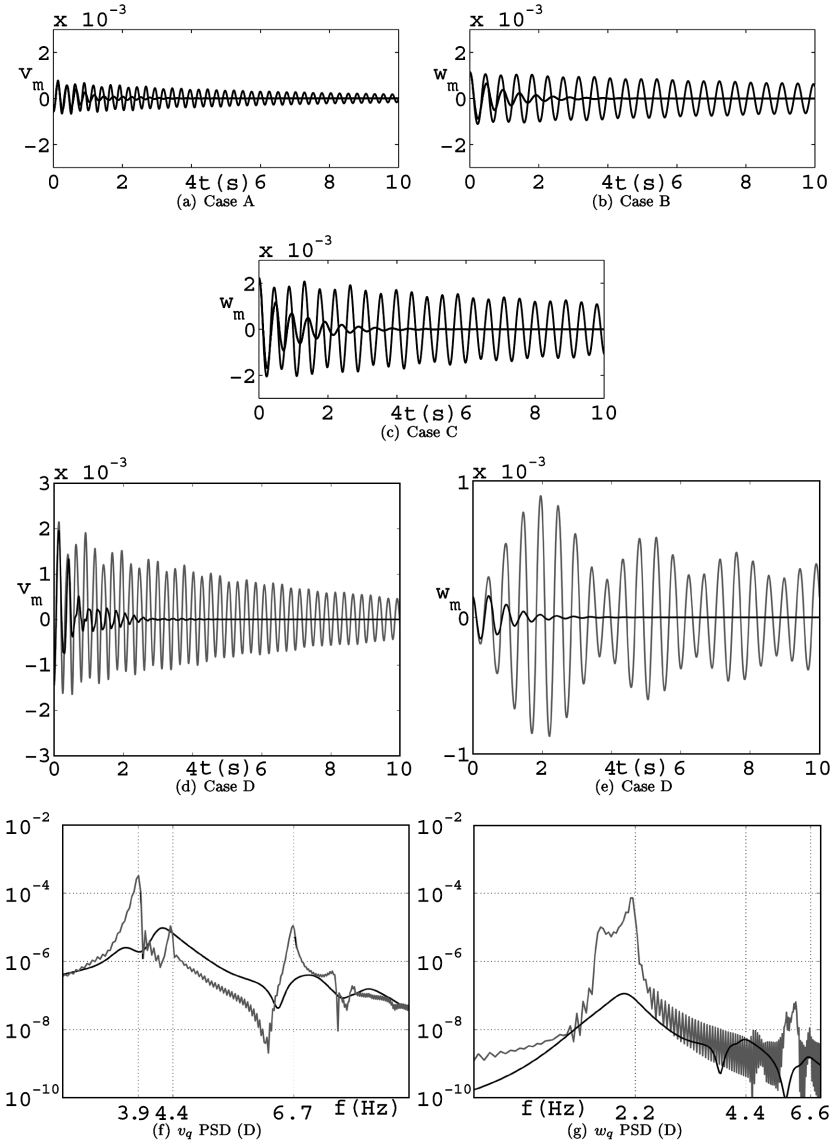

Fig. 4 Nonlinear free vibrations (uncontrolled in grey, controlled in black)

Table 4 Analysis cases for parametric harmonic excitation

Case	*E*	*F*	*G*
$\tilde{\Delta}x_0$	0.55	0.55	0.55
$\omega/\omega_1{}^y$	0.76	1.04	1.70

The amplitude Δx_0 of the imposed horizontal displacement is selected in such a way that the cable dynamics, under forced oscillations, is dominated by nonlinear phenomena, as described below. The excitation frequencies are such that: case *E* is between the 1:2 and the 1: 1 resonances with the first in-plane mode; case *F* is close to the primary resonance and case *H* is in resonance with the third in-plane

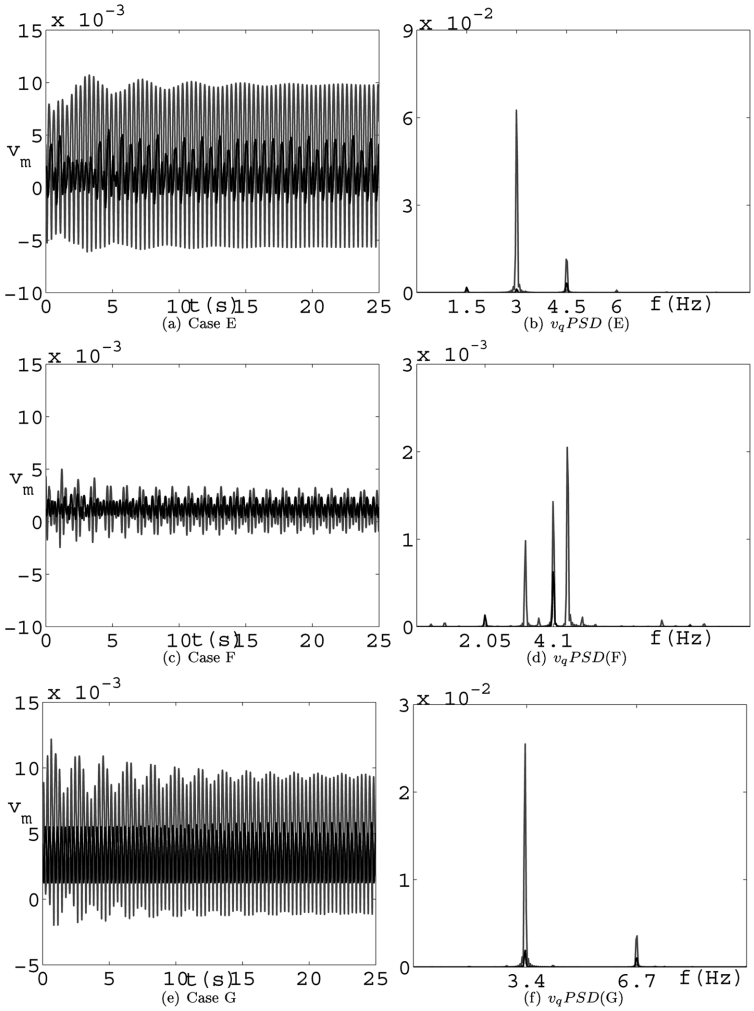

Fig. 5 Nonlinear vibrations under harmonic parametric excitation (uncontrolled in grey, controlled by black)

mode. Near zero initial conditions are assigned to the system in the three cases.

The results show that stable motions take place, after the initial transitory, in both uncontrolled and controlled cases. In particular, the control action is seen able to highly reduce the vibration amplitudes in all the considered cases. Large in-plane uncontrolled vibrations are observed in case *E*, due to the vicinity of the primary resonance (see Fig. 5(a)). The PSD of v_q in case *E* shows that the uncontrolled motion mainly posses the forcing frequency (f = 3Hz) plus a super-harmonic component f 3/2 and a sub-harmonic one f/2. In the controlled case the forcing peak and the super-harmonic one are drastically reduced, while the small sub-harmonic peak remains almost unchanged. In case *F* the cable motion is characterized by small vibration amplitudes. By varying the initial conditions, the cable would probably jump to a harmonic branch with larger vibration amplitudes. The uncontrolled motion, in such a case, is composed by the forcing frequency (f = 4.1Hz) and the two harmonics corresponding to the first two in-plane modes. A small sub-harmonic component f/2 is also detected. In this case, therefore, the uncontrolled response is quasiperiodic, since it contains incommensurate frequencies (i.e. their ratios

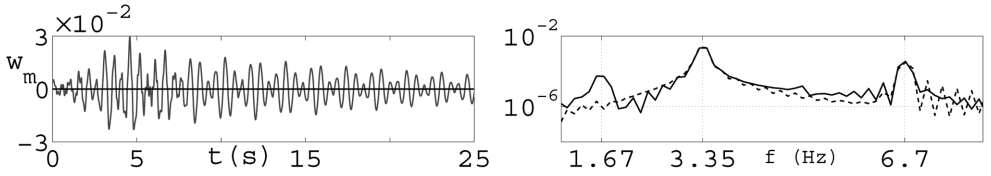

(a) Case G (b) Case G

Fig. 6 Out-of-plane vibration in case *G*: (a) PSD of controlled mid-span response v_m in case *G*, evidencing a period doubling bifurcation(the dashed line refer to the solution before the period doubling, the solid line refers to the solution after the period doubling) (b)

are irrational numbers). The controlled response, on the contrary, is periodic and contains the forcing frequency plus the sub-harmonic component $f/2$. In case *G*, a bifurcated spatial motion arises in the uncontrolled case (see Fig. 6a) , due to large in-plane vibrations caused by the resonance with the third in-plane mode. The control action reduces the in-plane vibrations and prevents such a bifurcation from occurring. However, a period doubling is evidenced in Fig. 5(e), in the controlled case, around $t = 8s$. This bifurcation is detected through the comparison of the PSD of v_m before and after the period doubling. The results are represented in Fig. 6(b) and show that the motion, before the period doubling, posses the forcing frequency and the sub-harmonic component $f/2$. After the period doubling, the sub-harmonic frequency $f/4$ appears. As it can be observed from Fig. 5(e), this bifurcation produces a small increment in the amplitude of vibration, when the cable under-goes positive (upwards) vertical displacements.

5. Application to an experimental cable model

5.1. Problem dimension reduction

The results presented above have shown, to some extent, that the MPD controller can be effectively employed for mitigating the response of shallow cables. By adopting a large dimensional FEM representation of the problem, it was also observed that control spillover did not arise if the weight matrix, in the Riccati equation, was properly chosen and a sufficient number of observations was exploited.

In control applications, accounting for only a few harmonics could result in serious inaccuracies (Johnson, *et al*. 2004). This happens since transversal control forces excite all the modes that have nonzero components at the location of the actuator. However, if higher modes are stabilized by the feedback control, their participation is kept small and , as a first approximation high order modes can be neglected. This point is evidenced in Fig. 7 where the root mean square (RMS) of the in-plane modal displacement is reported versus the mode number. The results refer to case *G* of forced parametric excitation, analyzed in Section 5. As inferable from such a figure, most of the energy is spread on the lower four modes in both the controlled and uncontrolled response. A small participation of some higher harmonics (between the 4-th and the 8-th modes) is observed in the controlled response. On the contrary, very high order modes (above the 8-th mode), do not essentially take part to the motion. This confirms that the dimension of the adopted FEM model (57 modes) is sufficient to accurately predict the controlled response.

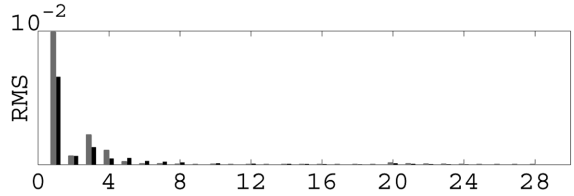

Fig. 7 RMS modal displacement vs. mode numbers in case *G* (uncontrolled response in gray controlled response in black)

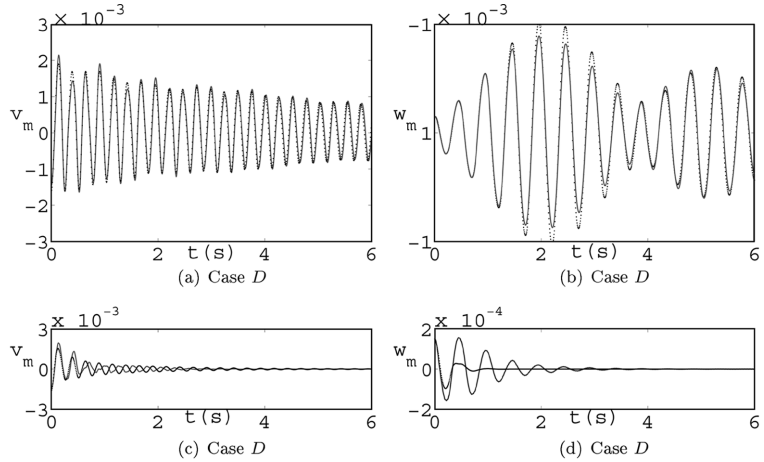

Fig. 8 Comparison between FEM (gray lines) and Galerkin (black dots) results under free spatial vibrations (Case *D*): uncontrolled response (a) and (b); controlled response (c) and (d)

Once it is ensured that high order modes do not strongly affect the behavior of the system, the reduction of the problem dimension can be performed. A very convenient way to do so, is to operate on the continuous model by means of the Galerkin approach described in Section 2.4.

The reduction of the problem dimension is particularly useful when operating in real time. Specifically, analytic Galerkin models result suitable for the design of linear and nonlinear state observers (Faravelli and Ubertini 2007). Within this framework, it can be shown that one in-plane and one out-of-plane observations are sufficient to construct the state observer, provided that the cable is not 1:1 in-plane internally resonant (Ubertini 2007).

Given the presented scenario, a Galerkin model with 4 in-plane and 4 out-of-plane degrees of freedom is adopted since, as observed above, it practically catches the whole dynamics of the system. As an example, the results of a comparison between FEM results and Galerkin results are reported in Fig. 8. The figure refers to case *D* of free spatial vibrations, analyzed in Section 4.4. Referring to the presented results, it must be observed that the uncontrolled responses, predicted by the two models, are practically equivalent, while some small differences (in both amplitudes and phases) are observed in the controlled case. This was however expected, due to the different way in which the feedback forces are calculated. In the FEM model, nodal interpolation is adopted to give heuristic estimates of the states, as already discussed in Section 4. In the analytic model, on the contrary, it is assumed that the states are known, which is technically meaningful since state observers can be adopted for the purpose.

Fig. 9 Experimental model of cable C_2

Table 5 Natural frequencies of cable C_2 normalized to the first in-plane natural frequency $f_{1s}^{y} = 4.4670$

In-plane modes	Analytical	F.E.M.	Out-of-plane modes	Analytical	F.E.M.
$\hat{f}_{1s}^{y}$	1.000	1.030	$\hat{f}_{1s}^{z}$	0.670	0.659
$\hat{f}_{1a}^{y}$	1.284	1.318	$\hat{f}_{1a}^{z}$	1.291	1.318
$\hat{f}_{2s}^{y}$	1.940	1.998	$\hat{f}_{2s}^{z}$	1.926	1.976
$\hat{f}_{2a}^{y}$	2.845	2.635	$\hat{f}_{2a}^{z}$	2.861	2.635

Table 6 Modal damping ratios of cable C_2 experimentally identified via wavelet analysis

In-plane modes	$2\xi_i$	Out-of-plane modes	$2\xi_i$
1s	0.0520	1s	0.0380
1a	0.0428	1a	0.0440
2s	0.0300	2s	0.0330
2a	0.0300	2a	0.0330

5.2. Experimental setup and model identification

A numeric application to an experimental model, called cable C_2, is presented as the result of this ongoing research. Although it is not properly and experimental verification, the numeric application to a physical model can give precious advices towards a real control experiment, which will be the object of future investigations.

The model is represented in Fig. 9 and it is characterized by the following non-dimensional parameters: $\mu = EA/H = 1242.8$ and $\nu = d/l = 0.0150$. The indicated parameters μ and ν, correspond to the stiffness non-dimensional Irvine parameter $\lambda^2 = 1.81\pi^2$, thus indicating that cable C_2 is placed on the left of the first crossover. The identification of cable C_2 has been reported elsewhere (Ubertini and Fuggini 2007), and led to the results summarized in Tables 5 and 6. A triaxial accelerometer, placed at $x = 0.75l$, has been used for identification purposes. The cable has also been monitored by means of two laser displacement sensors, placed at $x = 0.25L$ and a load cell to measure the dynamic horizontal tension $H(t)$. The measurements of the lasers have been adopted to confirm the results obtained by means of the accelerometer and to test their applicability in control applications. Since they directly measure the displacements, their implementation in state observation is straightforward. Two electromagnetic linear motors can be adopted as the control actuators (Casciati, *et al*. 2007).

The natural frequencies of the system have been determined by means of classic spectral analysis, while modal damping ratios have been measured via wavelet analysis. With such an approach, one can relate the damping ratio ξ_n, corresponding to the n-th mode, to the slope of the logarithm of the wavelet skeleton $|W_n|$. Without entering in deep details of the said approach, it must be mentioned that the

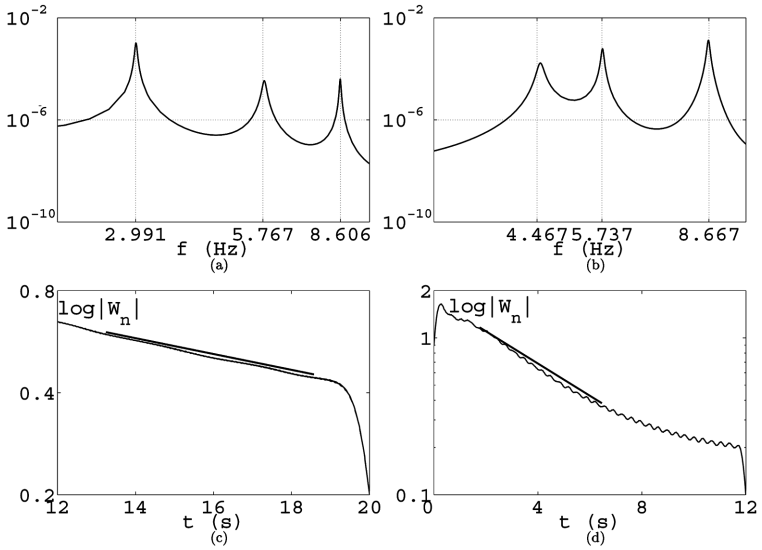

Fig. 10 Experimental results of cable C_2 identification: PSD of free out-of-plane acceleration (a); PSD of free in-plane acceleration (b); logarithm of wavelet modulus along the ridge corresponding to the first out-of-plane mode (c); logarithm of wavelet modulus along the ridge corresponding to the first in-plane mode (d)

wavelet skeleton is defined as the modulus of the wavelet transform W along the ridge identifying the n-th mode. Further details can be found in Staszewski (1997).

Fig. 10 reports some sample results of the system identification. Particularly, the PSD density functions of the cable in-plane and out-of-plane accelerations, measured by the accelerometer, clearly evidence the first six natural frequencies of the system. The corresponding wavelet skeleton of the first in-plane and out-of-plane modes are reported in Figs. 10(c) and (d). The results show that the logarithm of the wavelet modulus is approximately linear during the motion, which gives evidence of the physical meaning of modal viscous damping. The results also show the higher damping associated to the first in–plane mode with respect to the one associated to the first out-of-plane mode. The experimentally identified natural frequencies and modal damping ratios are summarized in Table 5 and 6. The natural frequencies of the continuous analytic model are also reported, from which a good accordance with experimental data can be observed.

5.3. Harmonic vibrations

A numeric analysis is performed, at first, to obtain the frequency response curves of the first in-plane and out-of-plane modes under harmonic excitation. This means that a harmonic input of normalized amplitude p=0.003 and frequency ratio ω/ω_1^y, enter the equation of the first in-plane of out-of-plane mode (see Eq. 5). Higher order modes are not retained at this preliminary stage.

The frequency response curves of the system have been obtained by means of an arclength continuation, implemented in a dedicated software (AUTO 2000 by Doedel, *et al.*) and are reported in Fig. 11. The results confirm the capability of the proposed approach to reduce the vibrations of the first two modes, in the highly nonlinear regime. In particular, a hardening behavior of the uncontrolled response around the primary resonance is evidenced in both the first in- plane and out-of-plane modes.

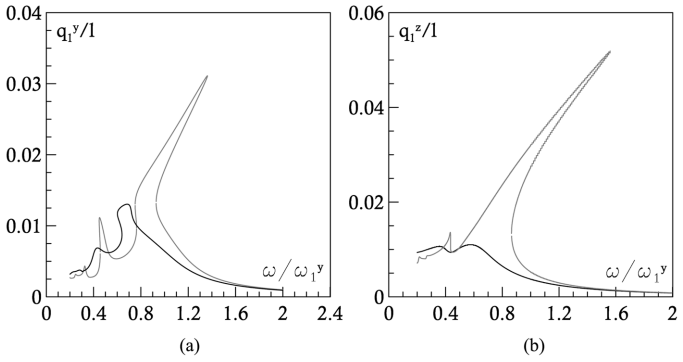

Fig. 11 Frequency response curves of cable C_2 (uncontrolled response in gray, controlled response in black): frequency response curve of the first in-plane mode under harmonic in-plane excitation with amplitude p=0.003; frequency response curve the first out-of-plane mode under harmonic out-of-plane excitation with amplitude p=0.003(b).

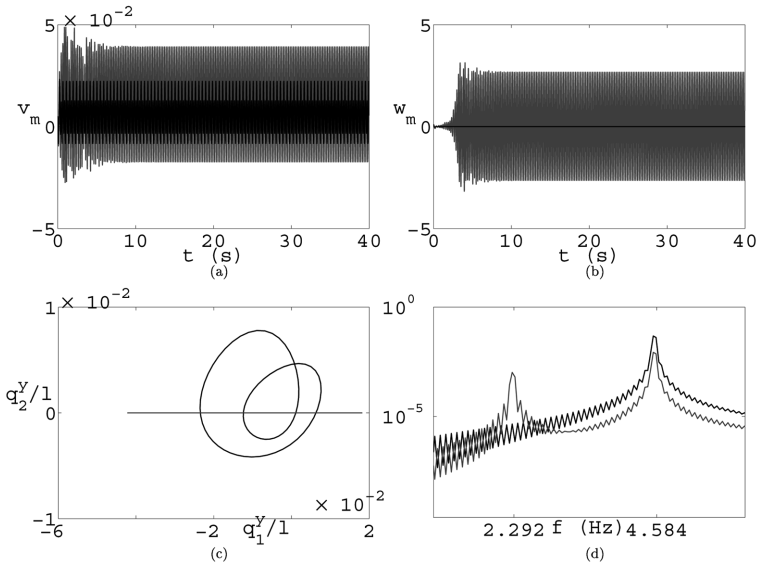

Fig. 12 Harmonic vibrations under in-plane loading ($\omega/\omega_1^y = 1$, $p = 0.005$): mid-span in-plane displacement (a); mid-apan out-of-plane displacement (b); phase plane projection (c); PSD of quarter-span in-plane displacement.

One-to-two ($\omega/\omega_1^y = 0.5$) resonant peaks are also observed, as expected, in the uncontrolled response. The control action introduces a significant additional damping in the system, leading to a strong reduction of the response. It must be mentioned, however, that the control action may locally increase the response with respect to the uncontrolled solution, such as, for instance, in the case of the first in-plane mode in the region around $\omega/\omega_1^y = 0.7$. This is a consequence of the frequency shift mainly produced by proportional terms in the control algorithm and of the softening behavior of the controlled response.

The resonant solutions ($\omega/\omega_1^y = 1$) obtained, for a larger amplitude $p = 0.005$, by means of the 8-dimensional Galerkin cable model, are reported in Figs. 12 and 13. In the case of forced in-plane vibrations (Fig. 12) a bifurcated spatial motion takes place in the uncontrolled case. The control action

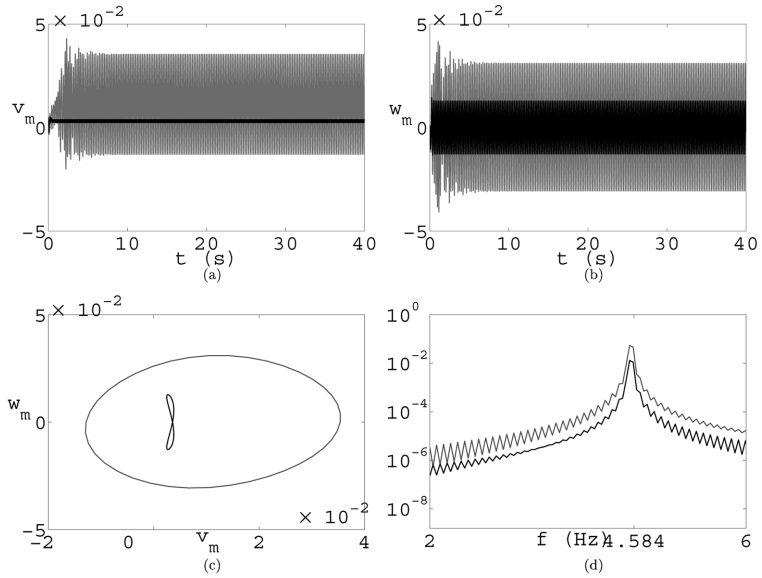

Fig. 13 Harmonic vibrations under out-of-plane loading ($\omega/\omega_1^y = 1$, $p = 0.005$): mid-span in-plane displacement (a); mid-span out-of-plane displacement (b); phase plane projection (c); PSD of quarter-span out-of-plane displacement

confirms its capability to stabilize the cable response in its plane. However, Fig. 12(c) shows that the second in-plane mode takes part to the motion in the controlled response, which is not the case in the uncontrolled one. This confirms that higher order modes may participate to the motion in the controlled case. Fig. 12(d) shows that the subharmonic frequency $f/2$ arises in the controlled in-plane harmonic response as a consequence of a period doubling bifurcation, $f = 4.584$ *Hz* being the forcing frequency. This fact has been already observed in Section 4 and confirms, to some extent, the capability of the adopted models to give similar results. The resonant forced out-of-plane harmonic solution is analyzed in Fig. 13. The results confirm that the control action is able to mitigate the spatial response of the cable. It must be observed that subharmonic frequencies do not arise in the out-of-plane response, which posses the only forcing frequency.

6. Conclusions

The mechanics of shallow cable vibration, with an active feedback controller, is numerically explored utilizing different methods. Derivative terms on the first two modes are analyzed, at first, in the framework of small displacements. Analytical explicit solutions are derived under free vibrations, in both uncontrolled and controlled cases. Higher order terms are then introduced in the control law, based on a linear quadratic regulator. A large dimensional geometric nonlinear FEM model is coded, to analyze the effectiveness of the control strategy and the stability of high order modes. The control action is seen able to reduce the cable vibrations in all the considered cases and to reduce out-of-plane bifurcations. Frequency analysis shows that sub-harmonic frequencies may arise in controlled harmonic vibrations. The modal participation, in relevant harmonic solutions, suggests the suitable dimension of a reduced Galerkin model of the controlled system. Afterwards, the model is applied to the controlled

dynamics of a physical suspended cable, arranged in the laboratory environment and identified for the purpose. The presented results constitute the theoretical basis towards an experimental investigation, which will be the major future development of this ongoing research.

Appendix

The linear free vibrations with MD control are analyzed in this section. The case of impulsive forces acting simultaneously at each node of the cable in the y and z directions at time t=0 is considered. The i-th modal equation of motion in the frequency domain, can be obtained from Eq. (10), (11) and (12) by adopting $g_{d1} = 0$ and by considering that the Laplace transform of the Dirac-delta function is the constant unit function:

$$\tilde{q}_i(s) = \frac{\tilde{A}_{\Delta i}}{s^2 + 2\xi_i\omega_i s + \omega_i^2} \tag{20}$$

where $\tilde{A}_{\Delta i} = A_{\Delta i}\sum_{j=1}^{3n}\Phi_{ji}$. Eq. (20) can be decomposed as follows:

$$\tilde{q}_i(s) = \left[\frac{A_i}{(s-a_i)} - \frac{A_i}{(s-b_i)}\right]\tilde{A}_{\Delta i} \tag{21}$$

where $a_1 = -\xi_i\omega_i + \omega_i\sqrt{\xi_1^2 - 1}$ is a complex value, b_i is its conjugate and $A_i = \frac{1}{a_i - b_i}$. Eq. (21) can be easily converted to the time domain by considering the properties of the Laplace transform. The following explicit formula can be derived to evaluate the uncontrolled solution in the time domain:

$$q_i(t) = [A_i e^{a_i t} - A_i e^{b_i t}]\tilde{A}_{\Delta i} \tag{22}$$

The overall cable response can be then calculated by modes superposition from Eq. (22).

The motion of the first, in-place or out-of-plane mode, with MD control, is described by Eq. (1). The modal amplitudes, in the time domain, can thus be calculated as described by Eq. (22)

By indication with the apices c the controlled solutions, it holds in particular:

$$q_1^c(t) = [A_1^c e^{a_1^c t} - A_1^c e^{b_1^c t}]\tilde{A}_{\Delta 1} \tag{23}$$

where $a_1^c = -\xi_1\omega_1 - \frac{\phi_1^0 g_{d1}}{2} + \omega_i\sqrt{\left(\xi_1 + \frac{\phi_1^0 g_{d1}}{2\omega_1}\right)^2 - 1}$ is a complex value, $b_1{}^c$ is its conjugate and $A_1^c = \frac{1}{a_1^c - b_1^c}$. The motion of the higher modes ($1 < j \le 3n$) is described by Eq. (8) which, in the frequency domain, becomes:

$$\tilde{q}_j^c(s) = \tilde{q}_j(s) - \phi_j^0 g_{d1}\tilde{A}_{\Delta 1}\left[\frac{A_j}{s-a_j} - \frac{A_j}{s-b_j}\right]\left[\frac{A_1^c}{s-a_1^c} - \frac{A_1^c}{s-b_1^c}\right]s \tag{24}$$

where $\tilde{q}_j^c(s)$ is the controlled solution and $\tilde{q}_j(s)$ is the uncontrolled one calculated with Eq. (21).

The expressions of A_j, a_j and b_j in Eq. (24) are the same as in Eq. (22), Eq. (24) can be converted back to the time domain as follows:

$$\tilde{q}_j^c(t) = q_j(t) - \phi_j^0 g_{d1} \tilde{A}_{\Delta 1} A_1^c A_j$$
$$\left[\frac{1}{a_j - a_1^c}(e^{a_j t} - e^{a_1^c t}) + \frac{1}{b_j - b_1^c}(e^{b_j t} - e^{b_1^c t}) - \frac{1}{a_j - b_1^c}(e^{a_j t} - e^{b_1^c t}) - \frac{1}{b_j - a_1^c}(e^{b_j t} - e^{a_1^c t})\right] \quad (25)$$

Acknowledgments

This paper was supported by FAR of University of Pavia, coordinated by Prof. Lucia Faravelli. The support of the Italian Ministry of University and Research (MIUR), within the PRIN projects grants is also acknowledged.

References

Abdel-Rohman, M. and Spencer, B. F. (2004), "Control of wind-induced nonlinear oscillations in suspended cables", *Nonlin. Dyn.,* **37**, 341-355.

Alaggio, R., Gattulli, V. and Potenza, F. (2006). "Experimental validation of longitudinal active control strategy for cable oscillations", *Proceedings of the 9th INVENTO Italian Conference on Wind Engineering,* Pescara, June.

Arafat, H. N. and Nayfeh, A. H. (2003), "Nonlinear responses of suspended cables to primary resonance excitations", *J. Sound Vib*., **266**, 325-354.

Benedettini, F., Rega, G. and Alaggio, R. (1995), "Nonlinear oscillations of four-degree of freedom model of a suspended cable under multiple internal resonance conditions", *J. Sound Vib*., **182**, 775-798.

Cai, C. S., Wu, W. J. and Shi, X. M. (2006), "Cable vibration reduction with a hung-on TMD system. Part I: Theoretical study", *J. Vib. Control*, **12**(7), 801-814.

Cai, C. S., Wu, W. J. and Shi, X. M. (2006), "Cable vibration reduction with a hung-on TMD system. Part II: Parametric study", *J. Vib. Control*, **12**(8), 881-899.

Casciati, F., Magonette, G. and Marazzi, F. (2006), *Technology of Semiactive Devices and Applications in Vibration Mitigation*, John Wiley & Sons, Chichester.

Casciati, F., and Ubertini, F. and Marazzi, F. (2007), "Nonlinear vibration of shallow cables with semi-active tuned mass damper", *Nonlin. Dyn*., in press, DOI 10.1007/s11007-007-9298-y.

Casciati, F., Fuggini, C. and Bonanno C. (2007), "Dual frequency GPS receivers: reliability of precision of the measures", *Proceedings of 4 colloque Interdisciplinaire en Instrumentation,* Nancy, October.

Cluni, F., Gusella, V. and Ubertini, F. (2007), "A parametric investigation of wind-induced cable fatigue", *Eng. Struct*., **29**(11), 3094-3105.

Doedel, E. J., Paffenroth, R. C., Champneys, A. R., Fairgrieve, T. F., Kuznetsov, Y. A., Oldeman, B. E., Sandstede, B. and Wang, X., *AUTO 2000: Continuation and bifurcation software for ordinary differential equations*, available online from http://indy.cs.concordia.ca/auto/.

Faravelli, L. and Ubertini, F. (2007), "Observability issues in the vibration of cables", *Proceedings of COMPDYN 2007 ECCOMAS Thematic Conference,* Crete, June.

Gattulli, V., Pasca, M. and Vestroni, F. (1997), "Nonlinear oscillations of nonresonant cable under in-plane excitation with a longitudinal control", *Nonlin, Dyn.*, **14**(2), 139-156.

Gattulli, V., and Vestroni, F. (2000), "Nonlinear strategies for longitudinal control in the stabilization of an oscillating suspended cable", *Dyn. Control,* **10**(4), 359-374.

Gattulli, V., Martinelli, L., Perotti, F. and Vestroni, F. (2004), "Nonlinear oscillations of cables under harmonic

loading using analytical and finite element models", *Comput. Meth. Appl. Mech. Eng.,* **193**, 69-85.
Hilber, H. M., Hughes, T. J. R. and Taylor, R. L. (1997), "Improved numerical dissipation for time integration algorithms in structural dynamics", *Earthq. Eng. Struct. Dyn*., **5**, 283-292.
Hui Li, Min, Liu and Jinping, Ou (2004), "Vibration mitigation of a stay cable with one shape memory alloy damper", *Structural Control Health Monit.*, **11**, 21-36.
Irvine, H. M. and Caughey, T. K. (1974), "The linear theory of free vibrations of suspended cables", *Proceedings of the Royal Society of London* **341**, 299-315.
Johnson, E. A., Christenson, RE. and Spencer, Jr., B. F. (2001), "Smart stay cable damping effects of sag and inclination", *Proceeding of '01 ICOSSAR,* Newport Beach, June.
Kolovsky, M. Z. (1996), *Nonlinear Dynamics of Active and Passive Systems of Vibration Protection,* Springer Verlag, Berlin.
Larsen, J. W. and Nielsen, S. R. K. (2004), "Non-linear stochastic response of a shallow cable", *Int. J. Non Lin. Mech.,* **41**, 327-344.
Luongo, A., Rega, G. and Vestroni, F. (1984), "Parametric analysis of Large amplitude free vibrations of a suspended cable", *Int. J. Solids Struct.,* **20**, 95-105.
Nayfeh, A. H., Arafat, H. N., Chin, C. M. and Lacarbonara, W. (2002), "Multimode interactions in suspended cables", *J. Vib. Control,* **8**, 337-387.
Pacheko, B. M., Fujino, Y. and Sulekh, A. (1990), "Estimation curve for modal damping in stay cables with viscous dampers", *ASCE J. Struct. Eng.,* **119**(6), 1961-1979.
Pasca, M., Vestroni, F. and Gattulli, V. (1998), "Active longitudinal control of wind-induced oscillations of a suspended cable", *Meccanica* **33**, 255-266.
Rega, G. (2004), "Nonlinear vibrations of suspended cables – Part I: modeling and analysis", *Appl. Mech. Rev.,* **57**, 443-478.
Rega, G. (2004), "Nonlinear vibrations of suspended cables – Part 2: deterministic phenomena", *Appl. Mech. Rev*., **57**, 479-514.
Soong, T. T. and Dargush G. F. (1997), *Passive Evergy Dissipation Systems in Structural Engineering,* John Wiley & Sons, Chichester.
Srinil, N. and Rega, G. (2007), "Two-to-one resonant multi modal dynamics of horizontal/inclined cables. Part I: Theoretical formulation and model validation", *Nonlin. Dyn.,* **48**(3), 231-252.
Srinil, N. and Rega, G. (2007), "Two-to-one resonant multi modal dynamics of horizontal/inclined cables Part II: Internal resonance activation, reduced order models and nonlinear normal modes", *Nonlin. Dyn.,* **48**(3), 253-274.
Staszewski, W. J. (1997), "Identification of damping in mdof systems using time-scale decomposition", *J. Sound Vib.,* **203**(2), 283-305.
Susumpow, T. and Fujino, Y. (1995), "Active control of multimodal cable vibrations by axial support motion", *Earthq. Eng. Struct. Dyn.*, **5**, 283-292.
The mathworks Inc (2002), Matlab and Simulink Natick MA.
Ubertini, F. and Domaneschi, M. (2006), "Analytic and numeric approach to controlled cables", *Proceedings of the 16th Italian Conference on Computational Mechanics* Bologna, June.
Ubertini, F. and Fuggini, C. (2007), "Confronto di due tecniche sperimentali per l'identificazione e il monitoraggio dei cavi strutturali" (in Italian), *Proceedings of AIPND conference*, Milano, October.
Xu, Y. L. and Yu, Z. (1999), "Non-linear vibration of cable damper system. Part I: formulartion", *J. Sound Vib.* **225**, 447-463.
Xu, Y. L. and Yu, Z, (1999) "Non-linear vibration of cable damper system. Part II: application and verification", *J. Sound Vib.* **225**, 465-481.
Wu, W. J. and Cai, C. S. (2006), "Experimental study of magnetorheological dampers and application to cable vibration control", *J. Vib. Control*, **12**(1), 67-82.
Zhou, Q. Nielsen, S. R. K. and Qu, W. L. (2006), "Semi active control of three dimensional vibrations of an inclined sag cable with magnetorheological dampers", *J. Sound Vib.,* **296**, 1-22.

FC